

NEBULOR Debris Removal Mission and JAV Deorbiting Method Concepts

Joshua B. Custard, Yehoshua N. Griver, Sasidhar Devabhaktuni, Zachary M. Kemper, Aditi Priya-Swaminathan, Shradul Sharma¹

Pennsylvania State University, University Park, PA, 16802, United States

Sara E. Lego²

Pennsylvania State University, University Park, PA, 16802 United States

Gregory R. Richardson³

Aerospace Corporation, Chantilly, VA, 20151, United States

As space is being used more, the accumulation of debris has become a growing problem. NEBULOR is the Venus Visionaries' design for the 2025 Cosmic Capstone Challenge that will help solve this problem. NEBULOR demonstrating the deorbit of Aerocube 6B, an inactive 0.5U CubeSat, by performing autonomous proximity operations with a suite of onboard sensors and deorbiting using the novel JAV. The suite and JAV form the payload of the BCT Venus bus that NEBULOR is based on. Unlike existing methods, the JAV does not pierce or attach to debris, instead hitting it to change its velocity. Considerations into power, GNC, propulsion, structure, thermal, communications, and C&DH systems, ground system, and launch vehicle are incorporated in the design to ensure it meets the requirements of the bus. Analysis of the payload and systems shows that it can meet requirements in pointing accuracy, data rates, structural support, power consumption, and payload mass and volume, though many requirements are yet to be verified. Recommended future work includes further analysis of system components, development of software to perform computer testing, and development of a JAV prototype for physical testing.

I. Introduction

Debris in low Earth orbit (LEO) has already significantly affected space operations. This is because, as pieces of debris collide, more debris is created, causing an exponential growth effect of the debris belt known as Kessler Syndrome [1]. This effect, combined with the increased number of spacecrafts in orbit, led NASA to predict that debris in LEO will be so numerous that orbits under 1000 km altitude will be impossible in only a few decades [2].

NEBULOR will demonstrate the use of the novel Junk Annihilation Vehicle (JAV) to deorbit Aerocube 6B. It accomplishes this by hitting debris to change the orbit instead of capturing or puncturing it, consuming only propellant for each deorbit. It is designed to be scalable to deorbit many types of debris, rather than focusing on one type like most methods outlined in the Catcher's Mitt study [3]. Venus Visionaries have a preliminary design of the JAV and how it works, detailing its necessary properties. In addition, the payload has onboard sensors for proximity operations on approach. This payload is supplemented by analysis of other spacecraft subsystems and mission elements necessary for such an operation.

II. Mission Overview

The NEBULOR mission will demonstrate the novel use of the JAV by deorbiting Aerocube 6B. Constraints from the RFP and safety of proximity operations defined most requirements for the mission. The Blue Canyon Technologies (BCT) Venus class satellite bus is the framework to hold standard subsystems and a specialized payload for proximity operations and the JAV. Success occurs if NEBULOR safely deorbits Aerocube 6B and does so autonomously.

¹ Student, Aerospace Engineering (jbc6331@psu.edu, yng5011@psu.edu, svd5858@psu.edu, zmk5164@psu.edu, amp7745@psu.edu, sjs7714@psu.edu)

² Associate Teaching Professor, Aerospace Engineering (ses224@psu.edu)

³ Principal Engineer, Civil Systems Group and Executive Director, COSMIC (gregory.g.richardson@aero.org)

A. Aerocube 6B

Aerocube 6B is a 0.5U CubeSat that was operated by the Aerospace Corporation but now is nonfunctional and considered debris. This was selected because its orbit was reasonably challenging to work with while it is a small mass, making the demonstration feasible but difficult enough to show rigor in the design.

It has perigee and apogee altitudes of 568 km and 627 km, respectively, inclination of 97.7°, and period of 96.5 minutes [4]. These values change often in low-Earth orbits, but they are useful for basic analysis. 97.7° is not purely polar, but it is enough to vastly change eclipse times throughout a year and make launch insertion more difficult.

B. Mission Process

For this mission, autonomous is defined as performing all necessary actions to move to the next mission phase given only initial instructions. NEBULOR will choose which actions to take, and it may use communications to obtain data. No human will decide when most communication occurs or tailor the information that is communicated. No instructions will be given outside of the initial set apart from noted exceptions.

This demonstration will follow the architecture in Fig. 1, which includes proximity operations. Operation of the JAV is discussed in Payload Design. NEBULOR will launch into an orbit near that of Aerocube 6B to initialize systems. The first phase is orbital rendezvous with Aerocube 6B. This is done using ground-based observation data consistently communicated to NEBULOR. Once Aerocube 6B is acquired with onboard sensors, it transitions to the next phase of proximity operations.

Proximity with onboard sensors shown in the dropout in Fig. 1. This details the sensors included and their maximum ranges. LiDAR is the only feasible sensor to detect the small CubeSat from 5 km range, but even this is still small compared to existing designs, so NEBULOR is more reliant on ground observations. Within 250 m, a narrow view optical camera can assist the LiDAR in tracking NEBULOR. Night operations are only possible with an infrared (IR) camera within 150 m, but this alone does not provide enough data for approach in night, so it is used only to keep track so the better sensors can resume in day. Stereoscopic cameras are used within 50 m to determine range more precisely and measure Aerocube 6B's spin rate so NEBULOR can match it. Though human input is not given, an observer must monitor operations to provide an abort command if necessary. The same observer ends this phase with manual verification to ensure systems are functioning before moving to deorbit.

The deorbit phase involves the JAV being launched at Aerocube 6B. The JAV will hit it, not pierce or capture it, to impart a change in velocity to deorbit it. Once sufficient velocity is imparted, NEBULOR will remain in a parking orbit to await another mission or use its systems to deorbit as part of its end of life (EOL).

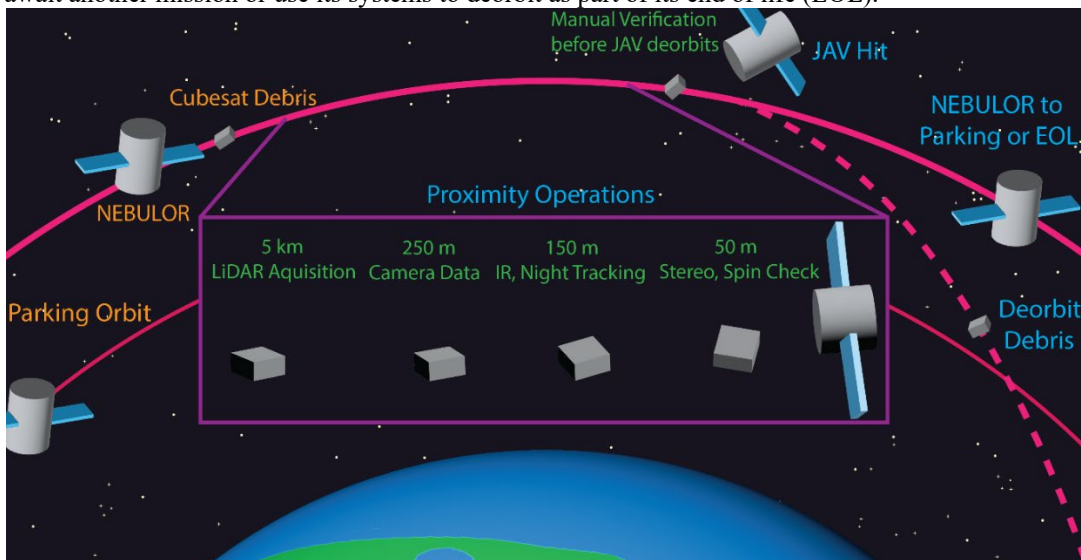


Figure 1. Overall NEBULOR Mission Architecture

C. Requirements

Main requirements are for the Venus class bus and come from the RFP. This includes payload volume and mass, spacecraft power production, and spacecraft power storage in a battery. Additional requirements were defined to ensure safe approach and deorbit of Aerocube 6B. Values are based on proximity operations studies, the JAV's method of deorbit, and regulations. System level requirements were defined for each phase of the mission during the system requirements review. Most of these are verified within this report. Key requirements are provided in Table 1.

Table 1. Top Level System Requirements

No.	Description	Source	No.	Description	Source
FR1.1	The payload shall have no more than 70 kg mass.	RFP, FR1	SR2.1	The payload shall track debris within 1 km and within 10% of the range.	[5], FR2
FR1.2	The spacecraft shall use no more than 10.2 Ah of stored energy.	RFP, FR1	FR3	The payload shall change the orbit when NEBULOR is within 10 m	[6]
FR1.3	The spacecraft shall use no more than 444 W of solar power.	RFP, FR1	RR4.1	Debris perigee shall be deorbited so it causes less than 10^{-4} casualties.	[7], SR4
FR1.4	The payload volume shall be smaller than 17" x 16.4" x 24"	RFP, FR1	RR4.2	Debris shall be deorbited in less than 5 years.	[8], SR4

D. Budgets

To ensure requirements for mass and power were fulfilled, budgets tables were made to calculate totals across the entire spacecraft. The values in the budgets are determined from specific components that could be included, heritage on similar designs, or mathematical analysis. Methods are outlined in Payload Design for the payload subsystems and in Host Spacecraft Integration and Mission Analysis for all other subsystems. Both budgets include a 20% margin on all values to account for variations later in design. The total payload mass is 24.6 kg and total spacecraft mass is 168 kg. Power is split between day and night to perform further analysis for night usage and battery recharging. The maximum expected is 282.7 W in day. The mass and power budget tables are shown in Table 2 and Table 3.

Table 2. Mass budget.

System	Mass	Units
Communications	20	kg
Propulsion	45	kg
GNC	5.5	kg
C&DH	1	kg
Structure	10	kg
Thermal	1.5	kg
Power	20	kg
Margin	20%	%
Bus Margin	20.6	kg
Bus Total	123.6	kg
System	Mass	Units
Structure	5	kg
JAV	8	kg
Prox Ops Suite	7.5	kg
Margin	20%	%
Payload Margin	4.1	kg
Payload Total	24.6	kg
Spacecraft Total	148.2	kg

Table 3. Power budget.

System	Day Min	Day Peak	Night Min	Night Peak	Units
Communications	0	26	0	26	W
Propulsion	0	5	0	5	W
GNC	7.4	37.6	7.4	7.4	W
C&DH	10	10	10	10	W
Structure	1	1	1	1	W
Thermal	25	75	25	75	W
Power	1	1	1	1	W
Bus Total	44.4	155.6	44.4	125.4	W
JAV	0	30	0	10	W
Prox Ops Suite	0	50	0	3	W
Payload Total	0	80	0	13	W
Margin	20%	20%	20%	20%	%
Margin	8.88	47.12	8.88	27.68	W
Spacecraft Total	53.28	282.72	53.28	166.08	W

E. Payload Overview

NEBULOR’s payload is split into two main components, the proximity sensor suite and the JAV. The proximity sensor suite is comprised of a LiDAR camera for long range acquisition, one narrow field of view (FOV) optical camera, an IR camera for night tracking, and two stereoscopic cameras for tracking and spin determination. These sensors have slightly overlapped ranges and capabilities to cover for deficiencies between them.

The JAV system is one of the most critical aspects of the NEBULOR mission and is capable of controlled deorbiting of Aerocube 6B debris. After NEBULOR has reached a leading-phase orbit with regard to the debris, the sensors are used to make proximity maneuvers to position within 10 m for the JAV. It then deploys the JAV via a calibrated spring mechanism, launched at 30 m/s. At impact, the JAV will hit the debris, without piercing or attaching to it and without damaging it. This imparts a change in velocity, lowering the debris’ perigee and expediting its atmospheric reentry. After impact, the tether on the JAV is reeled back in, resetting the system for subsequent missions if needed. This process facilitates repeated target impacts if needed to ensure the necessary adjustments are achieved.

This payload combines both proximity operations and deorbit capability to enable it to perform operations on various types of targets, regardless of if the target is compliant or not. The JAV in particular is a novel method of

deorbiting that did not appear even as consideration in research. Though loosely based on a harpoon, the fact it does not pierce or attach to the debris allows for the new method of operations without using NEBULOR’s propulsion system to deorbit. It also allows the system to be reusable many times because the only item consumed on the spacecraft is the propellant for orbital maneuvers.

III. Payload Design

Payload design was split to consider the proximity operations suite and JAV separately. The main consideration for integration of these subsystems was the distance from Aerocube 6B where the JAV will be used. It was decided that the JAV will have a long enough tether to hit Aerocube 6B while NEBULOR is at most 10 m away. If NEBULOR has a 0.01° pointing accuracy, as is given in proximity operations requirements, then the JAV will hit within 0.2 cm of the desired target, which was deemed accurate enough for the JAV requirements.

To meet system requirements, NEBULOR must impart the ΔV required to deorbit Aerocube 6B without creating more debris. This led to the payload design for the JAV mainly consisting of a balance between a high energy transfer capability while also not puncturing the debris in the process. This was achieved through the material selection of the JAV as well as a sufficient surface area that will impact Aerocube 6B. The sensor suite was designed to provide reliable data of Aerocube 6B’s relative position and orientation so NEBULOR can approach and align itself to use the JAV

Fig. 2 shows a 3D model of the payload without much structure, wiring, or thermal management. The JAV is secured within the chamber in the center to prevent undesired torques on NEBULOR when it is launched. It is pulled back into a spring to be launched by the winch at the bottom of the payload. A set of ceramic balls are used like bearings for alignment and reducing friction. The JAV is launched from the direct center so the launch does not impart a torque on NEBULOR. The sensors are arranged around the outside about the centerline. This is so the center of gravity stays near the JAV and so there is less deviation from the center to account for image processing. The big box at the top is LiDAR, the two smaller on its sides are stereoscopic cameras, and the two at the bottom are the IR camera and narrow view camera for long range. Fig. 3 shows specific dimensions in the three-view diagram.

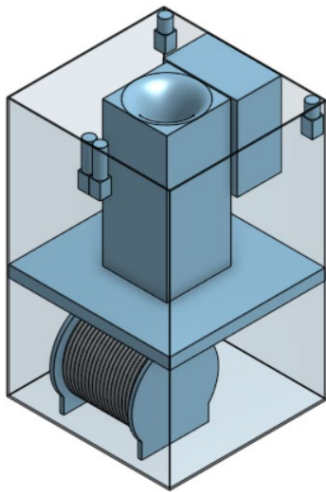


Figure 2. JAV Isometric View

The JAV itself is 17.4 cm in overall length, of which 2 cm consists of a silicone rubber impact surface and the remaining 15.4 cm of high-strength titanium alloy backing due to its optimum combination of hardness, density, and coefficient of thermal expansion. The projectile itself is 6 cm in diameter, significantly smaller than initially conceived during early design stages, a refinement that was the result of iterative impact and energy transfer simulations. Ball bearings of 2cm diameter were implemented as a low-friction solution for both launching and reeling the JAV back into place. The winch has a 19.7 cm drum length and 18 cm diameter to host a 15 m Kevlar tether. The stereoscopic cameras are separated as far as possible to improve depth perception which is critical to confirm alignment and impact effectiveness. The compactness of the JAV and the controlled release mechanism ensure that any deviation from the intended impact trajectory is minimal while maximizing the efficiency of the delta-v transfer to target debris.

Operation of the JAV begins once NEBULOR is within 10 m of Aerocube 6B and oriented properly. The spring begins to compress at the tail end of proximity operations so it can be used as soon as everything is in place. It is only compressed to the length necessary for the determined JAV launch velocity. When released, it launches the JAV to

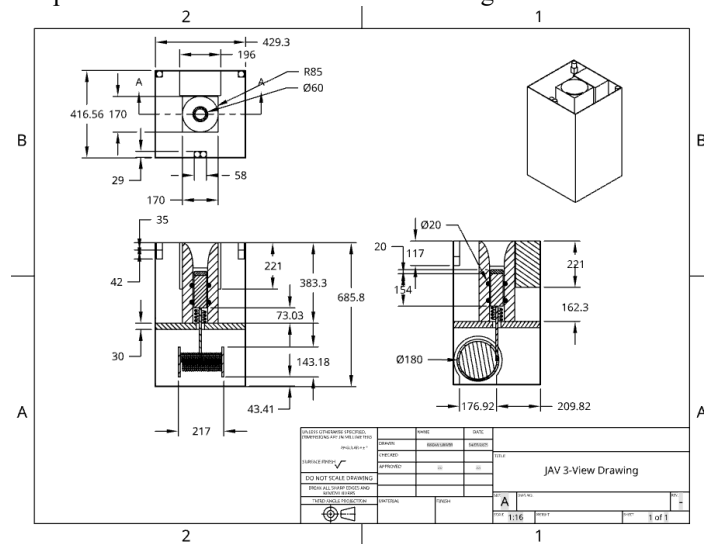


Figure 3. JAV 3-View Drawing

impact and transfer its momentum to Aerocube 6B. This will slow the debris down, reducing its perigee. It was determined that the JAV will have to make multiple impacts on Aerocube 6B to change the orbit to sufficiently reduce perigee. After each hit, the JAV will be reeled back in with its tether and the system will go back to proximity operations to reorientate the bus for additional hits. This process is shown in Fig. 4.

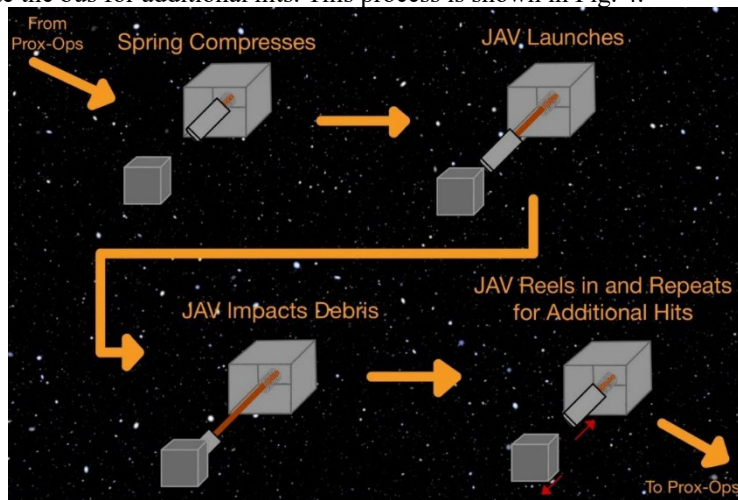


Figure 4. JAV mission architecture.

Once the bus is in the correct position relative to Aerocube 6B, the JAV process will begin with the spring compressing to the length necessary for the determined JAV launch velocity. Once properly compressed, the spring will be released, launching the JAV at Aerocube 6B. The JAV will impact Aerocube 6B and transfer its kinetic energy to it. This transferred energy will slow the debris down, changing its orbit. It was determined that for Aerocube 6B to reach the necessary transfer orbit for removal, the JAV will have to make multiple impacts with the debris. After each hit, the JAV will be reeled back in with its tether and the system will go back to proximity operations to reorientate the bus to be in the new orbit of the debris for additional hits.

A. Proximity Operations Payload Design

Design for the proximity suite began with deciding the main sensors to use. Three different pairs of sensors were considered for the suite: stereoscopic cameras with LiDAR, thermal imaging with radar, and a normal camera with hyperspectral sensor. A trade study was conducted to compare the three options considering the volume, mass, power, and maximum range of the sensor pairs. When the study was conducted, size, weight, and power were not tabulated for the whole spacecraft. Therefore, these were considered with equal importance since they still needed to be optimized. Range is also critical, so it was valued equally as well.

The trade study was done with the Analytical Hierarchy Process (AHP), where each category was weighted 25%. Values came from research into similar systems, and they were tabulated. The scoring was normalized from 0 to 1, where the worst design had 0 and the best had 1, and this depends on if the value is to be minimized or maximized. The results are shown in Table 4.

Table 4. Results of proximity operations suite trade studies.

Criteria	Weight	Goal	Stereo-Lidar	Radar-Thermal	Hyperspectral-Optical
Cuboid Volume (cm ³)	25%	MIN	2000	2000	1500
Normalized			0	0	1
Mass (kg)	25%	MIN	6.5	15	15
Normalized			1	0	0
Peak Power (W)	25%	MIN	17	35	30
Normalized			1	0	0.277777778
Range (km)	25%	MAX	50	5	50
Normalized			1	0	1
		Score	0.75	0	0.569444444

Stereoscopic cameras with LiDAR is definitively the best combination, so that is what the final concept worked with. Additionally, a narrow view camera was added to improve long range vision and an IR camera was added to allow limited operations in night.

The final concept combines several sensor types. Multiple are needed to cover all ranges, work at any light level, and obtain all necessary information. A list of the sensors is shown in Table 5, along with the data they measure and the method of measurement. Though they are not specifically designed for space, NASA has successfully modified a similar camera for space, so it should be feasible for these also [9].

Table 5. Sensors in proximity operations suite.

Sensor	Component	Range	Data	Method	Source
Far Field Optical Camera	1 Basler Ace U w/ 75mm Kowa Lens	50-250 m	Angles Only	Long exposure photography	[10],[11]
Stereoscopic Cameras	2 Basler Ace U w/ 35 mm Kowa Lens	0-50 m	Angles, Range, & Orientation	Image processing	[10],[12]
Infrared Optical Camera	1 Basler Ace Classic w/ 75 mm Kowa Lens	0-150 m	Angles Only	Long exposure photography	[13],[11]
Flash LiDAR	ASC GSFL-16KS	0-5 km	Range & Orientation	Active laser reflection	[14]

The camera for long range is necessary to acquire the target because of the pixel clarity needed to observe a 0.5U CubeSat from far away. LiDAR is difficult to use for acquisition because the lasers require precise pointing to use. Stereoscopic imaging allows all desired quantities to be measured with one system, so they are ideal for this. LiDAR is useful to supplement the stereoscopic cameras and to act as redundancy for range estimation if they fail.

These components are only effective in day, so an IR camera is added to observe Aerocube 6B's radiant heat at night. It is the only sensor added that is effective in night. It cannot support full operations, adding more sensors makes the payload too complex and power intensive. Therefore, it is used only to keep track in night, so operations can resume in day.

Once NEBULOR is in its parking orbit after launch, it will rendezvous using two-line element and direct ground observation data sent from the ground. NEBULOR is reliant on this information because its sensors only work at close ranges relative to orbit size. For this portion, data must be periodically sent from the ground, so this is not autonomous. When in maximum range, NEBULOR will point in the general area of Aerocube 6B using the data. Once it is confirmed that it is detecting Aerocube, autonomous proximity operations will begin.

To ensure it can rendezvous with only this data, analysis was performed by perturbing the true TLE set by up to 10%. With Keplerian motion, the positions between the true and perturbed set remained within 30 m of each other, so it is possible to reach the 6 km maximum sensor range.

The far range and IR cameras operate using long exposure images. Because NEBULOR is moving relative to the stars, they will appear as streaks in the images; however, Aerocube 6B will relatively be moving much less than the stars, so it appears as a smaller streak (or a dot if it is moving at the exact speed as NEBULOR). Processing shows Aerocube 6B's azimuth and elevation relative to NEBULOR, which can be integrated over time to determine range.

At closer range, the stereoscopic cameras take standard images to directly determine range and orientation. With the cameras separated by a known distance, the difference in the location of Aerocube 6B between the cameras can be used to determine the distance like humans do with their binocular eyes.

For the visible light cameras, this only works when Aerocube 6B is in daylight, as otherwise it would reflect no light. Additionally, NEBULOR must ideally be directly between the sun and Aerocube 6B so there are no shadows to reduce the visible portion of the already small CubeSat. Because eclipse times in LEO are short, IR radiation will still emanate from Aerocube 6B in night, so the IR camera can still be used then. With only one camera, though, it cannot perform full operations, instead simply keeping track until day again.

Orientation can be determined from image processing knowing the range and using optical fiducial. For Aerocube 6B, it was selected to use the golden colored piece on the top as the fiducial because it is distinct and decently high contrast to the metal surrounding it. This can be calculated at several times to determine spin rate of Aerocube 6b relative to NEBULOR.

In addition to the cameras, a LiDAR system was added for two reasons. First, the effective range of the cameras is extremely limited by the small size of Aerocube 6B, so much that it becomes unsafe to approach with the cameras alone. The LiDAR can detect more than 5 km away, which provides a large enough safety zone to acquire the target before approach. Second, its range estimation is much more accurate than with images. This accuracy is needed to meet requirements at longer ranges where the stereoscopic cameras are unusable.

Fig. 5 details the range and conditions each of these sensors are used throughout proximity operations. Note that the IR camera is the only sensor for night and is not usable at all ranges.



Figure 5. Ranges where sensors are used in proximity operations.

All sensors are currently in production by their respective manufacturers. Any physical data of them was also obtained by the manufacturer and applies only to the component itself without any connections or computation. The size, weight, and power are shown in Table 6. Note, stereoscopic cameras also require a separation distance as large as possible, but this is not added in the volume because it can be occupied by anything.

Table 6. Size, weight, and power of proximity operations sensors.

Component	Amount	Mass	Power	Volume	Source
Basler Ace U 75 mm Lens	1	90 g	2.8 W	29x29x117 mm	[10],[11]
Basler Ace U 35 mm Lens	2	90 g	2.8 W	29x29x77 mm	[10],[12]
Basler Ace Classic 75 mm Lens	1	90 g	2.6 W	29x29x117 mm	[13],[11]
Flash LiDAR	1	6.7 kg	40 W	11.7x19.6x22.1 cm	[14]
Total		7.06 kg	51 W		

For the cameras, the FOV, focal length, sensor resolution, and optical format are shown in Table 7. Focal length, resolution, and sensor format are provided by the manufacturer. The format is used to determine an approximate size of the sensor in mm, which is computed with focal length to determine FOV.

Table 7. Imaging properties of cameras.

Camera	FOV	Focal Length	Resolution	Sensor Format	Source
Basler Ace U 75 mm Lens	9.76x7.32°	75 mm	5472x3648	1"	[10],[11]
Basler Ace U 35 mm Lens	20.72x15.62°	35 mm	5472x3648	1"	[10],[12]
Basler Ace Classic 75 mm Lens	9.76x7.32°	75 mm	2048x2048	1"	[13],[11]

FOV shows how precise pointing must be for acquisition. The other quantities are used to calculate maximum range. This was determined by first choosing how many pixels Aerocube 6B would occupy on the sensor at that range. For far range and IR cameras, this is large enough to tell that an object is being seen instead of hot pixels. For stereoscopic cameras, it is larger because they are used for range and spin determination. This was related with the resolution, optical format, focal length, and actual size of Aerocube 6B to achieve the values in Table 8. Because the sensor is differently sized horizontally and vertically, the maximum distance depends on the direction, and so the minimum was taken. This was used to recalculate the pixels Aerocube 6B would actually occupy on the sensor. For all calculations, the 5 cm side of Aerocube 6B was used because its orientation in the camera can be any direction, and this accounts for minimum size.

Table 8. Maximum range and pixels occupied on sensor at that range.

Camera	Max Range	Chosen Pixels	Actual Pixels
Basler Ace U 75 mm Lens	356 m	4x4	4x4
Basler Ace U 35 mm Lens	66.5 m	10x10	11x10
Basler Ace Classic 75 mm Lens	150 m	4x4	4x4

For the long range and stereoscopic camera, the maximum operating range is less than the maximum possible range. This was reduced to ensure they can achieve proper clarity for first acquisition at long range and to take advantage of the stereoscopic effect at closer range. Because the IR camera is only used to keep track of Aerocube 6B in night, there is no reason to obtain more clarity than calculated.

The main requirement for proximity operations relates to range and error. The LiDAR maximum range and error are provided from the manufacture, being 6 km and 10 cm, respectively [14]. 6 km is far beyond the required 1 km, and the 10 cm error becomes 10% error at only 1 m, which is closer than is planned, satisfying the requirement. Still, the stereoscopic cameras are intended to have less error than this, though it is not verified if this is the case.

B. JAV Payload Design

Analysis of Aerocube 6B's orbit was performed to determine the ΔV necessary for deorbit. Debris at an altitude of 300 km experiences high atmospheric drag effects, enough that deorbit would occur within a few months for the NEBULOR missions targeted debris sizes. With the radius at perigee for Aerocube 6B and this targeted altitude of 300 km, the semimajor axis of the transfer orbit was found using Equation 1:

$$a_T = \frac{r_p + r_2}{2} \quad [1]$$

where a_T is the transfer orbit semimajor axis, r_p is the perigee radius of Aerocube 6B, and r_2 is the targeted radius for 300 km after the transfer. With the transfer orbit semimajor axis, the ΔV required for the orbit transfer was determined to be -88.6 m/s using Equation 2:

$$\Delta V = \sqrt{\frac{2\mu}{r_p} - \frac{\mu}{a_T}} - \sqrt{\frac{\mu}{r_p}} \quad [2]$$

where μ is the Earth's Gravitational Parameter, r_p is the perigee radius of Aerocube 6B, and a_T is the transfer orbit semimajor axis. This ΔV was used with the initial velocity of Aerocube 6B at perigee to find the velocity of Aerocube 6B needed for deorbit after the JAV hits. Conservation of momentum and energy, given as Equations 3 and 4, respectively, were then used to determine the JAV mass and JAV launch velocity:

$$m_a V_{a_1} + m_J V_{J_1} = m_a V_{a_2} + m_J V_{J_2} \quad [3]$$

$$\frac{1}{2} m_a V_{a_1}^2 + \frac{1}{2} m_J V_{J_1}^2 = \frac{1}{2} m_a V_{a_2}^2 + \frac{1}{2} m_J V_{J_2}^2 \quad [4]$$

where m_a is the mass of Aerocube 6B, m_J is the mass of the JAV, V_{a_1} is the velocity of Aerocube 6B before impact, V_{J_1} is the velocity of the JAV before impact, V_{a_2} is the velocity of Aerocube 6B after impact, and V_{J_2} is the velocity of the JAV after impact. These equations were chosen assuming that the collision would be perfectly elastic, although this assumption will be remedied with multiple hits. With these two equations, iterations over different possible JAV masses and the JAV launch velocity needed for these masses were performed to determine the optimal mass, the results of which are given in Fig. 6.

The initial JAV velocity shown is in the relative frame of Aerocube 6B and the bus. Since the bus will be in front of Aerocube 6B on its velocity vector, the relative velocity for the JAV is negative since it will be shot in the opposite direction of the bus's velocity. With smaller JAV masses, from about 0 to 2 kg, the initial JAV velocity to achieve the required ΔV is large. After reaching a JAV mass of about 2 kg, increasing the mass further does not have a large impact on the velocity that the JAV must be launched with, as the graph plateaus after this point. With this plot, it was determined that a JAV mass of 2 kg would be the best option, as it is on the lighter end while not requiring a much higher initial JAV velocity. For a 2 kg JAV, the initial relative velocity needed to achieve the determined Aerocube 6B ΔV is about -55 m/s.

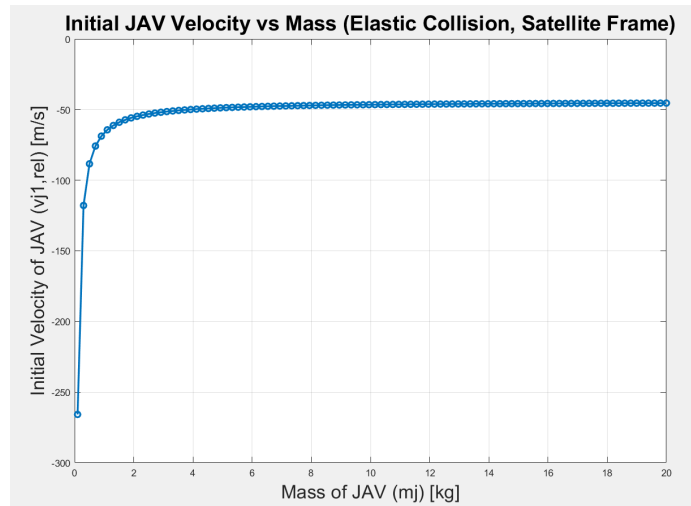


Figure 6. JAV Mass Analysis Graph

After determining the ideal JAV mass, the next decision was the material used for the JAV. As mentioned earlier, the JAV design must incorporate the idea of energy transfer to debris, but also the requirement of not creating further debris through breaking Aerocube 6B on impact. Avoiding damaging Aerocube 6B is accomplished by adding an elastic frontal impact surface, while achieving high energy transfer from the JAV to Aerocube 6B is fulfilled with a strong heavier density metal backing that makes up the bulk of the JAV volume. A trade study on material properties for different possible metal backings was performed to determine the best option, which is shown in Table 9.

Table 9. JAV main body material trade study results.

Criteria	Weight	Goal	Ti-6Al-4V	W-Ni-Fe	AISI 316 Stainless Steel
CTE ($\mu\text{m/m-K}$)	20%	MIN	8.6	6	16.2
<i>Normalized</i>			0.745098039	1	0
Density (g/cm^3)	20%	MIN	4.43	17	8.03
<i>Normalized</i>			1	0	0.713603819
Hardness (HRC)	15%	MAX	36	32	35
<i>Normalized</i>			1	0	0.75
Yield Strength (ksi)	15%	MAX	128	75	30
<i>Normalized</i>			1	0.459183673	0
UTS (ksi)	15%	MAX	138	110	75
<i>Normalized</i>			1	0.555555556	0
Youngs Modulus (ksi)	15%	MAX	16534	29000	27992
<i>Normalized</i>			0	1	0.919140061
Score			0.799019608	0.502210884	0.393091773

The titanium [15], tungsten [16], and steel [17] alloy options were chosen for their high strength and hardness. Due to the large span of operating temperatures that will be experienced in LEO, a low coefficient of thermal expansion was crucial for the mission, particularly in avoiding the degradation of the JAV over multiple hits. Along with this, it was determined that a material with a lower density was important to avoid damaging Aerocube 6B. With the fixed JAV mass selected, the density of the material determines the dimensions of the JAV as well. When made with a lower density metal, the volume of the JAV can be larger to fit the 2 kg mass, which then decreases its puncturing power.

The remaining properties, including hardness, yield strength, ultimate tensile strength, and Young’s modulus, were included to determine which alloy was best for avoiding JAV damage during impact. Each of these individual properties were less crucial to the primary goals of the mission, which is why they were given a lower weighting than the CTE and density. The titanium alloy (Ti-6Al-4V) was determined to be the best option for the JAV’s backing through this analysis, likely due to its combination of both a low CTE and density.

Though the titanium is useful to achieve proper mass, it is not ideal for impact because it is not so elastic. As such, a different material was selected to comprise the impact surface. Similar analysis was done for this material, the results of which are given in Table 10. This considers similar properties to the main body material, but the materials chosen for analysis and results reflect how these properties change value for this situation.

Table 10. JAV impact surface material trade study results.

Criteria	Weight	Goal	Polyurethane Rubber	Silicone Rubber	EPDM Rubber
CTE ($\mu\text{m/m-K}$)	15%	MIN	200	250	275
<i>Normalized</i>			1	0.333333333	0
Coefficient of Restitution	20%	MAX	0.65	0.55	0.8
<i>Normalized</i>			0.4	0	1
Tear Strength (kN/m)	15%	MAX	40	10	30
<i>Normalized</i>			1	0	0.666666667
Ductility	15%	MAX	4.5	5	3
<i>Normalized</i>			0.75	1	0
Glass Transition Temp. ($^{\circ}\text{C}$)	20%	MIN	-50	-110	-50
<i>Normalized</i>			0	1	0
UV Degradation (%)	15%	MIN	4	1	1
<i>Normalized</i>			0	1	1
Score			0.4925	0.55	0.45

The polyurethane [18], silicone [19], and EPDM [20] rubber were chosen for their high resistance to space conditions and ability to transfer energy. Glass transition temperature is the temperature that materials begin to transition from a rubbery state to become more brittle. Due to the very low operating temperatures reached in LEO, especially when in eclipse, the ability of the impact surface to remain flexible at low temperatures is an important property to consider. Additionally, the coefficient of restitution is another important aspect for successful deorbit, as this is a way to quantify the energy transfer from the JAV to Aerocube 6B. The other properties, including coefficient of thermal expansion, tear strength, ductility, and UV degradation all quantify the ability of the JAV impact surface to resist wear throughout operation. Silicone rubber was determined to be the best option for the JAV impact surface, although all three options were close in their rankings.

The cross-sectional area of the JAV was determined through a puncturing power analysis with Equation 5:

$$\frac{\frac{1}{2}mV^2}{A} \leq \sigma_y t \quad [5]$$

where m is the JAV mass, V is the JAV velocity at impact, A is the impact surface area, σ_y is the yield strength of Aerocube 6B's material, and t is the thickness of Aerocube 6B's impact surface.

The necessary impact surface area to avoid puncturing Aerocube 6B, including a factor of safety, was calculated and the corresponding JAV diameter was found. Finally, the length of the JAV's metal backing was determined with the mass, material densities, and cross-sectional area.

In addition to the JAV properties, the spring for launching and tether for reeling back in were determined. As mentioned earlier, the required launch velocity of a 2 kg JAV for complete deorbit is about -55 m/s for Aerocube 6B. Reaching this velocity with one launch would require a spring that is unrealistic for implementation for the NEBULOR mission, which is why it was determined that multiple hits will be needed to achieve the total ΔV . The JAV launch velocity that could be achieved for different springs was found by rearranging to solve for velocity in Equation 6:

$$\frac{1}{2}mV^2 = \frac{1}{2}kx^2 \quad [6]$$

where m is the mass of the JAV, V is the launch velocity of the JAV, k is the spring constant of the spring, and x is the compression distance of the spring. After analyzing the launch velocities possible for springs that would fit within the payload, the best option was determined to be the LHL 2000D 01 spring, which has a compression length of 0.0635 meters and a spring constant of 437817 N/m, which can be used to achieve a launch velocity of about 29.71 m/s [21]. With this spring, two JAV hits will be enough to achieve the needed ΔV . All calculations of JAV velocity were made assuming no losses during launch or impact, although performing multiple hits will be enough to correct for these losses. A braided Kevlar tether will be attached to the JAV for reeling back in. A braided tether was chosen for its good strength-to-weight ratio and high tensile strength. Since the JAV will be launched 10 meters away from Aerocube 6B, the tether will be made 15 m long so that it remains slack during the launch and impact. The necessary cross-sectional area and diameter of the tether was found using Equations 7 and 8:

$$F = m \frac{\Delta V}{\Delta t} \quad [7]$$

$$\sigma = \frac{F}{A} \quad [8]$$

where F is the shock force applied to the tether, m is the mass of the JAV, ΔV is the change in velocity if the tether becomes slack, Δt is the impact time, σ is the tensile strength of the tether, and A is the tether cross-sectional area. The shock force was calculated, which was then used with the tensile strength of braided Kevlar and a factor of safety of 4 to find a minimum tether diameter of 3 mm. The tether diameter was set to 1 cm, which will provide sufficient resistance to shock forces while also being small enough to fully wrap around the winch within the bus. Additional analysis must be carried out to verify that the tether can withstand the space environment, including ultraviolet radiation exposure.

To ensure that the JAV hits Aerocube 6B at the correct location, an alignment system was implemented to maintain the pointing accuracy. This system consists of two rows of three ceramic balls surrounding the JAV while it is sitting within the bus. These balls will be encapsulated by the structure of the walls surrounding the JAV, with the ends on the outside of the wall touching the JAV itself. These balls will be free to spin during launch and spring compression, which allows the JAV to operate without much frictional effects from the alignment system. Ceramic composite material was determined to be ideal for these balls to avoid material expansion during the fluctuation temperatures that it will be exposed to. To ensure that the balls have minimal frictional effects on the JAV, a space grade PFPE lubricant will be used with the balls to ensure they are able to spin freely. Additional analysis of this method of alignment is required to verify that it will provide the necessary pointing accuracy to the JAV, which would consist of building and testing a computer model of the ball system.

IV. Host Spacecraft Integration and Mission Analysis

Design work, analysis, and trade studies were conducted within each of the remaining subsystems to ensure they meet requirements. Also included in this work is analysis for the ground system and launch. Work performed here was used to generate the mass and power budget tables.

A. Power

The power subsystem is planned to be comprised entirely from the standard components included in the Venus bus. This includes the two-panel array, which produces 444 W, and a 10.2 Ah battery. It is planned to run most components at standard 28 V, but transformers are likely needed to reduce voltage, especially for the proximity operations sensors.

Power for each subsystem was tabulated in Table 3 to ensure it would not exceed 444 W, including a 20% added margin to all values to account for changes later in design. The values come from analysis on all subsystem components or heritage, and they show a maximum usage of 282.7 W. To further verify that NEBULOR has enough power, a full power profile was developed using eclipse data of Aerocube 6B generated by the Ansys STK for a full year starting June 1, 2025. This accounts for excess power to charge batteries and need to shut down to minimum power if the battery begins to die. Assumptions include 200 W maximum input or output from the battery, an 80% maximum depth of discharge on the battery, and a sinusoidal variance of power between the maximum and minimum, chosen to be reasonable but ultimately arbitrary. This showed that it is possible to accommodate the current budget with 48% efficiency on the 444 W panels. Results of this analysis for some of the longest eclipses are shown in Fig. 7. Net power, in black, is the difference between required and available power, which never goes below zero.



Figure 7. Power profile for longest elcipse periods.

B. Guidance, Navigation, and Control

The guidance, navigation, and control (GNC) subsystem analyzed also includes the attitude determination and control system (ADCS). The GNC subsystem is comprised of Microsat components manufactured by BCT, NewSpace, and Beyond Gravity. It includes star trackers for determining attitude, reaction wheels and torque rods for control, and a computer to manage the wheels and rods. A list is provided in Table 11.

Table 11. GNC subsystem components for analysis.

Component	Name	Manufacturer	Amount	Mass	Power	Volume	Source
Star Tracker	Standard NST	BCT	2	0.35 kg	3.5 W	10x5x5.5 cm	[22]
Reaction Wheel	RWP 500	BCT	4	0.86 kg	6 W	112x124x38 mm	[23]
Torque Rod	NCTR-M016	New Space	3	60 g	1.2 W	107x15x13 mm	[24]
Computer	CODE	Beyond Gravity	1	1.1 kg	3 W	190x125x58 mm	[25]
Total				5.26 kg	37.6 W		

Components selected come from BCT when possible because they should more easily be integrated into the BCT Venus bus. From BCT components, a gimballed control moment gyro (CMG) would have less mass and power overall, but reaction wheels are preferred. Momentum must be stored and released constantly in all directions during proximity operations, and a CMG is less efficient and fast to do this than dedicated reaction wheels in each direction. Additionally, the CMGs made by BCT have not been flight tested, but there are 700 of their reaction wheels currently on orbit [23][26].

Torque rods were added to the system to despin the reaction wheels from the Earth's magnetic field without consuming propellant. They are the only way to despin. Only standard star trackers were chosen because of power considerations. The CODE is intended for step motors, like in thrusters or antennae, but this can be adjusted for the continuous reaction wheel motors. An additional star tracker and reaction wheels are added as redundancy. In particular, the fourth wheel will be oriented between the other three, which will be aligned along the principal axes. In this configuration, if any one wheel fails, the mission can still proceed.

The reaction wheels will all be controlled by the CODE using a control algorithm that takes input from attitude data from the ground during rendezvous and from sensor data during proximity operations. This algorithm has not been designed, so it is unclear if NEBULOR will meet requirements for maintaining its spin rate. When not in proximity operations, the torque rods will be used to despin the reaction wheels. Although this is limited by Aerocube

6B’s polar orbit, NEBULOR will be near the equator often enough to utilize Earth’s magnetic field. BCT’s Flexcore system, which this is based on, has 0.002° pointing accuracy [27]. Though the pointing accuracy of launching the JAV is not determined, the accuracy of the ADCS system provides margin for analysis of the current alignment mechanism.

C. Command & Data Handling

The Command and Data Handling (C&DH) system is one of the major subsystems of the NEBULOR mission, responsible for command execution, data flow control, and ensuring smooth coordination between onboard components. For the NEBULOR mission, we have selected the ISIS iOBC onboard computer, along with MRAM and Flash memory for storage, and I2C, UART, and SPI communication interfaces. These components were selected based on the low power, high reliability, and radiation tolerance requirements, which are necessary to ensure the success of the mission in the space environment.

The ISIS iOBC was chosen as the onboard computer due to its flight heritage, low power (~1 W typical, 1.5 W peak), and range of interfaces (I2C, UART, SPI). This 400 MHz ARM9 core-based processor with 64 MB RAM and 2 GB Flash storage has sufficient computational power to handle telemetry, process mission commands, and interface with payload subsystems. Its built-in error detection and correction also enhance reliability, ensuring system stability in a radiation-prone environment. The onboard MRAM (16-64 MB) is used for critical data retention, offering non-volatile storage with radiation tolerance, well suited to maintain important mission parameters even in the event of a power cycle. The Flash memory (2 GB) is used as backup storage, employed primarily for long-term telemetry and mission logs.

The communications interface was customized for data flow efficiency optimization with power consumption considered. I2C (3.4 Mbps, 0.1 W) serves as the system bus and interconnects major subsystems such as power management, GNC, and sensors, providing low-power, multi-device communication. For telemetry transmission and debugging, UART (1 Mbps, 0.05 W) is a simple, robust data link. An SPI interface (50 Mbps, 0.2-0.5 W) is reserved for high-speed payload data transfer to allow mission-critical sensor data to be efficiently processed and relayed. Together, these protocols provide strong, redundant, and power-efficient communication with reduced risk of data loss or transmission error.

The C&DH components and their respective specifications are shown in Table 12.

Table 12: C&DH Subsystem Components

Component	Specifications	Rationale for Selection	Source
Onboard Computer	ISIS iOBC (400 MHz ARM9, 64 MB RAM, 2 GB Flash, 1.5 W max)	Low-power, flight-proven, radiation-tolerant	[28]
Primary Storage	MRAM (16-64 MB, radiation-resistant, 0.5 W)	Ensures critical data retention, fast access	[29]
Backup Storage	Flash (2 GB, onboard iOBC, 0.3 W)	Stores mission telemetry & logs	[30]
Primary Bus	I2C (3.4 Mbps, 0.1 W)	Efficient low-power subsystem communication	[31]
Telemetry Link	UART (1 Mbps, 0.05 W)	Reliable debugging & backup data link	[32]
High-Speed Data	SPI (50 Mbps, 0.2-0.5 W)	Enables rapid sensor and payload data transfer	[33]

This architecture provides a robust, low power, and fault-tolerant C&DH system capable of meeting the command execution, telemetry, and subsystem coordination needs of the mission within tight power and reliability constraints. Future system integration testing and fault tolerance testing will be performed to ensure that the C&DH system is qualified to fulfill all the mission needs before launch.

D. Thermal Subsystem

The thermal subsystem for the NEBULOR mission is responsible for maintaining operational and survival temperatures of components within the bus. Since the JAV operations will occur in direct sunlight, a matte white paint coating will be applied to the bus. This provides a high emissivity surface, which allows for greater emission of spacecraft generated heat, while also providing a lower absorptivity to lower the heat transfer from the sun to the bus. With this coating in mind, heat transfer to the bus is modeled with Equation 9:

$$q_{solar} + q_{albedo} + q_{planetshine} + Q_{gen} = Q_{stored} + Q_{out,rad} \quad [9]$$

Where q_{solar} is the solar heating, q_{albedo} is the planet reflection solar heating, $q_{planetshine}$ is the planet infrared heating, Q_{gen} is the heat generated by the bus, Q_{stored} is the stored heat by the bus, and $Q_{out,rad}$ is the heat emitted from the bus through radiation [34]. The values of q_{solar} , q_{albedo} , and $q_{planetshine}$ were estimated using typical heating values in LEO, while Q_{gen} was found using typical smallsat generated heat values. Assuming the bus is in

thermal equilibrium, Q_{stored} can be estimated as zero. These heat transfer values were used to solve for the radiative heat transfer in direct sunlight, which can also be written as Equation 10:

$$Q_{out,rad} = \epsilon\sigma AT^4 \quad [10]$$

With the emissivity and absorptivity of the white coating, the surface area of the bus, and the calculated radiative heat transfer, the maximum temperature within the bus when in sunlight was found to be 87.21 °C. The minimum temperature during eclipse was found using the same equations but setting q_{solar} and q_{albedo} to zero, which was calculated to be -39.17 °C.

Along with the calculated bus temperatures, the operating and survival temperature ranges for the components used within the bus for the NEBULOR mission were determined, as shown in Table 13.

Table 13: Minimum and Maximum Operating Temperatures for Components [35]

Component	Operational (°C)	Survival (°C)
Battery	0 to 15	-10 to 25
Reaction Wheels	-10 to 40	-20 to 50
Torque Rods	-30 to 80	-40 to 85
Star Trackers/LiDAR	0 to 30	-10 to 40
Computers	-30 to 65	-40 to 75
Hydrazine Tanks/Lines	15 to 40	5 to 50
Antennas	-100 to 100	-120 to 120
Solar Panels	-150 to 110	-200 to 130

Additional thermal control is required to keep the components within these required temperatures. The methods of temperature control that will be implemented within the bus consist of passive and active systems, including multi-layer insulation (MLI) blankets, radiators, a variable conductance heat pipe (VCHP), electrical heaters, and thermoelectric coolers. MLI blankets are ideal for reducing temperature fluctuations, which is beneficial for avoiding excessive heat loss in eclipse and heat gain in direct sunlight. Radiators implemented onto the bus will dissipate excess generated heat by the components, which is ideal when the bus is in sunlight. A VCHP passively regulates heat throughout the bus, avoiding extreme temperature differences. Electrical heaters and thermoelectric coolers are active systems that are used to heat and cool components, respectively.

Components with stricter temperature ranges, including the battery, star trackers, and LiDAR, require individual thermal control systems to remain within operating temperatures. A combination of a thermoelectric cooler and electrical heater will be implemented with the battery to remain at the operating temperature range at all points on the orbit. The payload operations will occur in sunlight, which allows the cameras to be within the survival range instead of the operational range during eclipse. Due to this, the star trackers and cameras will be integrated with MLI blankets for temperature regulation during all phases as well as thermoelectrical coolers for operation in sunlight. The hydrazine tanks require higher minimum temperatures than other components, so an electrical heater will also be used to keep within this range. The overall bus temperature will be controlled with an MLI blanket coating on the inside of the bus, as well as with the radiators and a VCHP system throughout the bus. The combination of these three passive components will be enough to maintain the ranges for the remaining components.

E. Structure Subsystem

The structural subsystem for the NEBULOR mission ensures that the bus will not fail under the loads experienced during operation, most notably the vibrations during launch. While the bus is attached to the launch vehicle, the bending mode can be approximated with a cantilever beam model. With this assumption, the fundamental frequency that the bus yields to during launch is estimated with Equation 10:

$$f_n = \frac{1}{2\pi} \sqrt{\frac{3EI}{ML^3}} \quad [11]$$

where f_n is the fundamental frequency, E is the modulus of elasticity, I is the area moment of inertia of the bus, M is the mass of the bus, and L is the length from the root to the center of mass. To mitigate the effects of vibratory loads on the bus, an aluminum alloy 6061 chassis with honeycomb panels will be implemented onto the payload. The high strength to weight ratio and corrosion resistance of aluminum alloy 6061 makes it an ideal material for the chassis, while the honeycomb structure of the panels provides high vibrational damping [36]. With this chassis in mind, the fundamental frequency that the bus will yield to during launch was calculated to be about 87.32 Hz. This fundamental frequency was used in Equation 11 to find the load factor that the bus must withstand during launch.

$$LF = \sigma \left[\frac{\pi}{4} (PSD) \vartheta f_n \right]^{0.5} \quad [12]$$

Where LF is the load factor, σ is a safety factor, PSD is the power spectral density of acceleration, ϑ is the percent critical damping, and f_n is the fundamental frequency. Using values from our launch vehicle, the load factor was found to be 24.8 g's of acceleration [37]. This load factor was used to find the stress that the bus would experience both axially and laterally, which was 16917.5 Pa and 10275.6 Pa, respectively. Assuming the bus material is aluminum with a yield strength of about 11 MPa, the yield strength can be compared to the calculated stresses experienced by the bus. Including a factor of safety, the bus with the chassis will easily be able to withstand the vibrations experienced during launch.

After reaching the orbit of Aerocube 6B, the loads experienced by the bus will be much lower than those during launch but will still be monitored with sensors. The majority of these in-orbit loads will be experienced specifically by the JAV system during operation. As discussed earlier, the JAV payload was designed to avoid failure from these loads, including both the impact surface during hit and the tether withstanding shock loads from becoming taut.

F. Propulsion Subsystem

The propulsion subsystem on NEBULOR is designed to provide adequate thrust for orbital maneuvers, attitude control will be handled by on-board torque rods and wheels, and the controlled transitions during proximity operations. The system is based on a monopropellant hydrazine architecture due to its high reliability, heritage in spacecraft applications, and compatibility with small satellite platforms such as the BCT Venus bus. NEBULOR is planned to carry about 39 kg of hydrazine. The mass is arbitrary because no analysis has been carried out for NEBULOR's maneuvers, but it should be high to allow more missions. Hydrazine is useful because it is a monopropellant and so only needs one tank. Hydrazine's density of approximately 1.01 kg/L results in a minimum tank volume of 49.5 L, with a margin included to accommodate pressurization and thermal expansion effects. The propellant is stored in a Northrop Grumman PM-80304-1 Diaphragm tank, which can store all the hydrazine and is flight-proven [38].

Thrust is provided by four Aerojet Rocketdyne MR-103 g monopropellant thrusters. Each capable of producing up to 1.13 N of thrust with a specific impulse of 215 s [39]. These offer sufficient thrust for maneuvers, close-approach operations, and EOL disposal. With this configuration, NEBULOR can adjust its orbit autonomously during each mission phase while maintaining compliance with system-level requirements and safety margins.

G. Communication Subsystem

The communication subsystem facilitates dependable bidirectional data transfer between the spacecraft and mission control, which is essential for telemetry, command execution, and payload management in LEO. It utilizes a dual-band transceiver that operates on S-band (2.2 GHz) for low-data-rate telemetry and X-band (8.4 GHz) for high-data-rate transmissions, reaching speeds of up to 100 kbps. This setup enables real-time transmission of sensor data from debris-tracking payloads [40]. The antenna system features a Honeywell S-Band Transceiver [41] with a phased-array configuration for omnidirectional coverage, alongside a Ball Aerospace Multi-Band, Multi-Mission (MBMM) antenna [42] equipped with a two-axis gimbal for accurate X-band downlink targeting. Link timings are optimized for brief ground station visibility windows (5–15 minutes per orbit).

Redundancy is emphasized to address potential single-point failures, incorporating backup transponders, power converters, and automatic failover systems. In the event of misalignment of the primary high-gain antenna, control is transferred to the phased-array system, thereby maintaining continuous operations. Ground operators can issue contingency commands through S-band to reset hardware or reconfigure the subsystem in response to anomalies. The design complies with a link budget, effectively balancing performance, global coverage, and cost efficiency to fulfill the requirements of LEO debris removal missions. This architecture aligns with industry standards for fault tolerance in space systems, ensuring the success of missions even in the face of component failures [43].

H. Ground Station

The ground system of the Swedish Space Corporation (SSC) plays a important role in facilitating dependable communication, tracking space debris, and executing commands throughout the mission. This system utilizes SSC's Erange and Kiruna ground stations as its foundational infrastructure, supplemented by redundant power systems and adaptive transceivers to enhance reliability and coverage. This design effectively balances high-performance capabilities, regional reach, and cost-effectiveness, featuring a link budget that provides robust margins to support critical mission activities.

The 15-meter antennas utilized by SSC at Erange and Kiruna form the essential communication infrastructure for the mission. These installations operate at S-band (2.2 GHz for uplink) and X-band (8.4 GHz for downlink)

frequencies, which have been chosen for their efficient atmospheric penetration and their common application in LEO missions [44].

The uplink from the SSC ground stations transmits commands to the spacecraft using a 250 W transmitter for each antenna, totaling 500 W for two antennas, which are equipped with 15-meter dishes. This configuration yields an effective isotropic radiated power (EIRP) of 30.17 dB, adequately addressing the characteristics of the spacecraft's receiving antenna. The uplink budget is calculated based on a slant range of 1,200 km, which accounts for the space loss that the system is engineered to mitigate. Despite the presence of atmospheric absorption, the link retains a sufficient margin to guarantee reliable command transmission during spacecraft maneuvers or in situations where signal obstructions may occur.

The downlink utilizes the high-gain antenna of spacecraft, which provides a gain level that the SSC system is specifically engineered to recognize. The ground stations of the SSC are equipped with 15-meter receiving antennas that deliver gains of 28.66 dB and maintain low system noise temperatures of 1000 K. This capability enables the detection of signals even in the presence of space loss at a frequency of 8.4 GHz. Consequently, this setup creates a margin that supports high-data-rate telemetry at 100 kbps for payload operations, encompassing real-time tracking of debris and implementing collision avoidance strategies. Table 15 provide the summary of the link budget of both the uplink and downlink for the SSC ground station.

Table 14. Link Budget Summary of SSC Ground Station

Parameter	Uplink	Downlink
Frequency	2.2 GHz (S-band)	8.4 GHz (X-band)
Transmitter Power	250 W each (500 W total)	5 W (6.99 dBW)
Antenna Gain	24.18 dB	28.66 dB
Space Loss	-160.87 dB	-172.51 dB
Margin	3.27 dB	4.83 dB

I. Launch Vehicle

The Rocket Lab Neutron has been selected as the launch vehicle for the NEBULOR mission due to its compatibility with mission requirements, including ESPA ring integration, retrograde orbit insertion capability, and cost efficiency [37]. As a reusable medium-lift rocket with a carbon composite structure, Neutron provides an optimal balance of performance and sustainability. Neutron's ESPA ring compatibility ensures seamless payload integration, simplifying mission planning. Its ability to support customized launch profiles makes it well-suited for inserting NEBULOR into a retrograde orbit, a maneuver requiring additional energy beyond standard prograde launches. Neutron's payload capabilities provide ample margin for this requirement. A key advantage of Neutron is its flexibility in scheduling dedicated launches, avoiding the constraints of traditional rideshare options. While a new vehicle with first flights set for 2025, Rocket Lab's track record with Electron demonstrates strong reliability.

Cost considerations also played a role in the selection. While ULA's Vulcan Centaur and Arianespace's Ariane 6 were evaluated, Neutron offers a cost-effective alternative without sacrificing performance. Its partially reusable architecture further reduces expenses, making it a financially viable option. Before finalizing the launch contract, structural load analysis and launch environment verification will be conducted to ensure compatibility. Launch availability will be confirmed, and contract negotiations with Rocket Lab will align the mission budget and schedule. With dedicated launch capabilities, ESPA ring compatibility, and retrograde orbit support, Neutron is the most suitable option for the NEBULOR mission.

V. Risk and Fault Recovery

To further the design for implementation, all systems were analyzed to identify things that would be more likely to fail or disastrous if they failed. Of these, the four most dangerous shown in the risk analysis matrix in Fig. 8 were changed to mitigate the risk. A is for the JAV striking the incorrect part of Aerocube 6B, B is for LiDAR failure, C is for the tether snapping, and D is for a proximity collision between NEBULOR and Aerocube 6B. The arrows denote how they changed before and after mitigation.

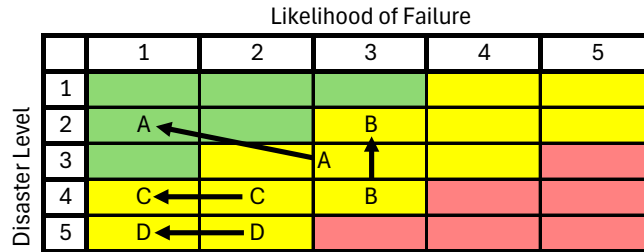


Figure 8. Risk analysis matrix. Arrows show direction of change after mitigation.

The way each was mitigated is described in Table 16. If the JAV hits Aerocube 6B improperly, it may induce a torque on it or damage equipment which may release debris. Mitigation involved computing pointing error between the ADCS and JAV launcher to see if it was below 0.01° . ADCS accuracy is 0.002° , but JAV accuracy is unknown, though a method of alignment is proposed. LiDAR is the only sensor that can be used at safe range for acquisition. Without it, NEBULOR must utilize the reduced radial safety zone of satellites to use the 250 m camera in several passes above and below debris until enough data is found to approach at 250 m. If the JAV tether snaps, it would mean mission failure since NEBULOR could no longer deorbit anything. The tether material and size was considered and stress calculated to ensure it would not break. When doing proximity operations, there is always a risk of colliding with the target. To avoid this, sensors are used where they can obtain more data. Moreover, an observer will monitor proximity operations to provide a manual abort command if necessary.

Table 15. Risk mitigation methods.

Risk	Mitigation Method
JAV Hit Misaligned	Develop a pointing error budget between all systems and verify budget.
LiDAR Failure	Inclusion of long-range optical camera to allow modified approach.
JAV Tether Snapping	Analyze fracture of tether and reduce JAV maximum launch speed to reduce stress.
Proximity Collision	Operate sensors below maximum range to ensure more accurate data.

Even with the risk reduced, descope options were developed for if the tether snapped or LiDAR failed. If the tether snaps, it is no longer possible to deorbit anything. However, if the proximity sensors are still functional, the mission can instead only be about proximity operations and observation rather than the dual approach that also includes deorbit. This is mission failure, but it would allow partial use of NEBULOR.

If the LiDAR fails, the planned leading in-line approach would become too dangerous because the maximum range of the cameras is only 250 m. This distance is not enough to acquire Aerocube 6B and slow down and is well outside the in-line safety zone of any satellite. However, the radial and tangential safety zones of satellites are much smaller, though the zones for Aerocube 6B were not determined. A modified approach with NEBULOR being radially above and below Aerocube 6B can be possible, but this will require many passes above and below to properly locate Aerocube 6B before making a safe approach. Normal operations can continue from this point.

VI. Future Work

The current iteration of NEBULOR represents a nearly comprehensive conceptual design with basic analysis across all major spacecraft subsystems. However, several areas remain for further development before the mission can be advanced towards full-scale implementation. Future work will focus on refining subsystem designs, validating assumptions through high-fidelity modeling, and integrating system-level considerations such as launch environment and long-term reliability. This work can be used for the Preliminary Design Reivew.

Testing will include the development of computer models and physical prototypes for testing. Particularly, a prototype of the JAV and spring launch is crucial to account for nonideal energy transfer, which was not accounted for in analysis. This can validate momentum transfer assumptions and ensure structural integrity through repeated collisions. The spring and tether mechanisms must also be tested in a vacuum to ensure alignment and friction do not impact it. Orbit modeling for both debris and NEBULOR should include perturbations from a variable atmospheric drag model, such as MSIS, to validate long-term deorbit trajectories. This will ensure a more informed budget for velocity changes on the debris and will work towards refining NEBULOR's propulsion subsystem.

Proximity sensors must be tested for space applications and code for image processing must be developed. Furthermore, algorithms must be developed between proximity sensors, ADCS, and propulsion systems to allow for autonomous approach.

Generally, all spacecraft subsystems need more refinement and requirement verifications, especially those not in the payload. The risk descope options will be formalized into operational procedures. Across all subsystems, mass and power budgets will continue to be refined as component selections are finalized.

References

- [1] Kessler, D. J., and Cour-Palais, B. G., "Collision Frequency of Artificial Satellites' The Creation of a Debris Belt," *Journal of Geophysical Research*, Vol. 83, No. A6, 1978, pp. 2367–2646.
- [2] Goddard Space Flight Center. "On-Orbit Satellite Servicing Study," NASA. NP-2010-08-162-GSFC. October 2010.
- [3] Pulliam, W., "Catcher's Mitt Final Report," DARPA, AD1016641. <https://apps.dtic.mil/sti/pdfs/AD1016641.pdf>. Accessed 5 April, 2024.
- [4] "AEROCUBE 6B," N2YO. <https://www.n2yo.com/satellite/?s=40046>. Accessed 7 April 2025.
- [5] Barbee, B. W., Carpenter, J. R., Heatwole, S., Markley, F. L., Moreau, M., Naasz, B. J., and Eepoel, J. V., "Guidance and Navigation for Rendezvous and Proximity Operations with a Non-Cooperative Spacecraft at Geosynchronous Orbit," NASA. <https://ntrs.nasa.gov/api/citations/20100019266/downloads/20100019266.pdf>. Accessed 7 April 2025.
- [6] Pulliam, W., "Catcher's Mitt Final Report," DARPA, AD1016641. <https://apps.dtic.mil/sti/pdfs/AD1016641.pdf>. Accessed 7 April 2025.
- [7] Federal Aviation Administration, "§ 450.101 Safety Criteria," Title 14 Aeronautics and Space, <https://www.ecfr.gov/current/title-14/chapter-III/subchapter-C/part-450/subpart-C/section-450.101>. Accessed 7 April 2025.
- [8] Rosenworcel, Starks, and Simington, "Second Report and Order. FCC Adopts New '5-Year Rule' for Deorbiting Satellites to Address Growing Risk of Orbital Debris," Federal Communications Commission. FCC 22-74. September 2022. <https://docs.fcc.gov/public/attachments/FCC-22-74A1.pdf>. Accessed 7 April 2025.
- [9] NASA Technology Transfer Program, "Ruggedized Infrared Camera," NASA, <https://technology.nasa.gov/patent/MFS-TOPS-108>. Accessed 7 April 2025.
- [10] Basler, "Basler ace U acA5472-5gc," <https://www.baslerweb.com/en-us/shop/aca5472-5gc/>. Accessed 7 April 2025.
- [11] Basler, "Kowa Lens LM75HC F1.8 f75mm 1", " <https://www.baslerweb.com/en-us/shop/kowa-lens-lm75hc-f1-8-f75mm-1/>. Accessed 7 April 2025.
- [12] Basler, "Kowa Lens LM35HC F1.4 f35mm 1", " <https://www.baslerweb.com/en-us/shop/kowa-lens-lm35hc-f1-4-f35mm-1/>. Accessed 7 April 2025.
- [13] Basler, "Basler ace Classic acA2040-25gmNIR," <https://www.baslerweb.com/en-us/shop/aca2040-25gmNIR/>. Accessed 7 April 2025.
- [14] Advanced Scientific Concepts, "GSFL-16KS Space 3D Flash LiDAR," https://asc3d.com/gsfl_16ks/. Accessed 7 April 2025.
- [15] "Titanium Ti-6Al-4V (Grade 5), Annealed," ASM Aerospace Specification Metals Inc. Available: <https://asm.matweb.com/search/SpecificMaterial.asp?bassnum=MTP641>. [Accessed 15 March 2025].
- [16] "Tungsten Alloy Physical and Chemical Properties as per ASTM B777-15," Ed Fagan Inc. Available: <https://heavy-metal-tungsten-alloy.com/tungsten-alloy-physical-chemical-properties.php>. [Accessed 15 March 2025].
- [17] "AISI 316 Stainless Steel Properties, SS 316 Grade Density, Composition, Yield Strength, Thermal Conductivity," World Material. Available: <https://www.theworldmaterial.com/316-stainless-steel/>. [Accessed 15 March 2025].
- [18] "Polyurethane (EU/AU)," Minnesota Rubber & Plastics, Trelleborg. Available: <https://www.mnrubber.com/tools-resources/design-guide/elastomers-materials/polyurethane/>. [Accessed 15 March 2025].
- [19] "Silicone Rubber," AZO Materials. Available: <https://www.azom.com/properties.aspx?ArticleID=920>. [Accessed 15 March 2025].
- [20] "All About EPDM Rubber – Properties, Applications, and Uses," Arvico Rubber. Available: <https://www.arvicorubber.com/epdm-rubber-properties/>. [Accessed 15 March 2025].
- [21] "HEFTY Die Springs," Lee Spring. Available: <https://www.leespring.com/compression-springs-hefty>. [Accessed 15 March 2025].
- [22] Blue Canyon Technologies, "Nano Star Trackers," <https://www.bluecanyontech.com/components/nano-star-trackers/>. Accessed 7 April 2025.
- [23] Blue Canyon Technologies, "Reaction Wheels," <https://www.bluecanyontech.com/components/reaction-wheels/>. Accessed 7 April 2025.
- [24] NewSpace, "Magnetorquer Rods," https://www.newspacesystems.com/wp-content/uploads/2021/10/NewSpace-Magnetorquer-Rod_20211018a.pdf. Accessed 7 April 2025.

- [25] Beyond Gravity, “Core Drive Electronics,” https://www.beyondgravity.com/sites/default/files/media_document/2023-11/BG-CODE.pdf. Accessed 7 April 2025.
- [26] Blue Canyon Technologies, “Control Moment Gyroscopes,” <https://www.bluecanyontech.com/components/control-moment-gyroscopes/>. Accessed 7 April 2025.
- [27] Blue Canyon Technologies, “Flexcore,” <https://www.bluecanyontech.com/components/flexcore/>. Accessed 7 April 2025.
- [28] ISISPACE, “On-Board Computer,” <https://www.isispace.nl/product/on-board-computer/>. Accessed 8 April 2025.
- [29] Mouser Electronics, “Everspin MRAM,” <https://www.mouser.com/new/everspin-technologies/everspinmram/>. Accessed 8 April 2025.
- [30] Provantage, “Juniper Networks SRX600-2GB-CF 2GB Compact Flash Memory Module,” Provantage, <https://www.provantage.com/juniper-networks-srx600-2gb-cf~7NSCN0LU.htm>. Accessed 8 April 2025.
- [31] I2C.info, “I²C Bus Specification,” I2C.info, <https://i2c.info/i2c-bus-specification>. Accessed 8 April 2025.
- [32] Texas Instruments, “Universal Asynchronous Receiver/Transmitter (UART),” Texas Instruments, <https://www.ti.com/lit/ug/sprugp1/sprugp1.pdf>. Accessed 8 April 2025.
- [33] Microchip Technology Inc., “Serial Peripheral Interface (SPI),” Microchip Technology Inc., <https://ww1.microchip.com/downloads/en/devicedoc/spi.pdf>. Accessed 8 April 2025.
- [34] “Thermal Control,” NASA, February 2024. <https://www.nasa.gov/smallsat-institute/sst-soa/thermal-control/>. Accessed 8 April 2025.
- [35] Larson, W. J. and Wertz, J. R., *Space Mission Analysis and Design*, Microcosm Press, California and Kluwer Academic Publishers, Boston, 1999.
- [36] “Aluminum 6061, Al 6061-T6 Alloy Properties, Density, Tensile & Yield Strength, Thermal Conductivity, Modulus of Elasticity, Welding,” World Material. <https://www.theworldmaterial.com/al-6061-t6-aluminum-alloy/>. Accessed 8 April 2025.
- [37] ROCKETLAB, “Payload Users Guide,” Rocket Lab USA, <https://www.rocketlabusa.com/assets/Uploads/Rocket-Lab-Neutron-PUG-reduced-final.pdf>. Accessed 8 April 2025.
- [38] Northrup Grumman, “PMD Tanks Data Sheet – Sorted by Volume,” <https://www.northropgrumman.com/space/pmd-tanks-data-sheets-sorted-by-volume>. Accessed 8 April 2025.
- [39] Aerojet Rocketdyne, “Monopropellant Rocket Engines,” L3 Harris, https://www.l3harris.com/sites/default/files/2023-07/AJRD-LHX_Monopropellant_Rocket_Engines_SpecSheet_CMYK_061423_APPROVED.pdf. Accessed 8 April 2025.
- [40] Leonardo DRS, “What are S- and X-band radar and how are they used today?,” <https://www.leonardodrs.com/news/thought-leadership/what-are-s-and-x-band-radar-and-how-are-they-used-today/>. Accessed 10 April 2025.
- [41] Satsearch, “S-Band TT&C Transceiver STC-MS03,” <https://satsearch.co/products/honeywell-aero-s-band-tt-c-transceiver-stc-ms03> Accessed 10 April 2025.
- [42] Nyirady, A. “Lockheed Martin Completes Phased Array Test With Ball Aerospace, Wins SDA Contract,” *Satellite Today*. “<https://www.satellitetoday.com/government-military/2020/09/02/lockheed-martin-completes-phased-array-test-with-ball-aerospace-wins-sda-contract/>” Accessed 10 April 2025.
- [43] Johnson Space Center. “Pressurized Payloads Interface Requirements Document: International Space Station Program,” NASA. SSP 57000. October 2015.
- [44] “Our Stations,” Swedish Space Cooperation. “<https://sscspace.com/services/satellite-ground-stations/our-stations/>”. Accessed 10 April 2025.